

Supplementary Information

Sigma Receptor Ligands Carrying a Nitric Oxide Donor Nitrate Moiety: Synthesis, In-Silico, and Biological Evaluation

Emanuele Amata,^{†,§,*} Maria Dichiara,^{†,§} Davide Gentile,[‡] Agostino Marrazzo,[†] Rita Turnaturi,[†] Emanuela Arena,[†] Alfonsina La Mantia,^{||} Barbara Rita Tomasello,^{||} Rosaria Acquaviva,^{||} Claudia Di Giacomo,^{||} Antonio Rescifina,[‡] Orazio Prezzavento^{†,*}

[†]Department of Drug Sciences, Medicinal Chemistry Section, University of Catania, Viale A. Doria, 95125 Catania, Italy.

[‡]Department of Drug Sciences, Organic Chemistry Section, University of Catania, Viale A. Doria, 95125 Catania, Italy.

^{||}Department of Drug Sciences, Biochemistry Section, University of Catania, Viale A. Doria, 95125 Catania, Italy.

Corresponding Authors:

*E.A.: phone, (+39) 0957384102; email, eamata@unict.it.

*O.P.: phone, (+39) 3396392909; email, prezzave@unict.it.

Author Contributions:

[§]E.A. and M.D. contributed equally.

EXPERIMENTAL SECTION

Table of contents

Chemistry	S2
General details	S2
Synthesis of compounds 5–8	S2
Synthesis of compounds 9–20	S3
Synthesis of compounds 23a and 23b	S6
Computational procedures	S6
Molecular docking	S6
Molecular optimization	S8
Molecular dynamics simulations	S8
Molecular dynamics simulations study and trajectories analysis of compound 18	S8
Biological evaluation	S10
Radioligand binding assays	S10
Detection of Nitrite: Griess Reaction	S11
Cell culture	S11
Cell viability	S11
Western Blot Analysis	S12
NMR spectra	S13
References	S18

Chemistry

General details

Reagent grade chemicals were purchased from Sigma-Aldrich (St. Louis, MO, USA) or Merck (Darmstadt, Germany) and were used without further purification. All reactions involving air-sensitive reagents were performed under N₂ in oven-dried glassware using the syringe-septum cap technique. Flash chromatography purification was performed on a Merck silica gel 60 (40-63 μm; 230-400 mesh) stationary phase. Nuclear magnetic resonance spectra (¹H NMR recorded at 200 and 500 MHz) were obtained on VARIAN INOVA spectrometers using CDCl₃, DMSO-*d*₆, or CD₃OD. TMS was used as an internal standard. Chemical shifts (δ) are given in parts per million (ppm) and coupling constants (*J*) in Hertz (Hz). The following abbreviations are used to designate the multiplicities: s = singlet, d = doublet, t = triplet, q = quartet, quint = quintet, m = multiplet, br = broad. The purity of all tested compounds, whether synthesized or purchased, reached at least 95% as determined by microanalysis (C, H, N) that was performed on a Carlo Erba instrument model E1110; all the results agreed within ± 0.4% of the theoretical values. Reactions were monitored by thin-layer chromatography (TLC) performed on 250 μm silica gel Merck 60 F₂₅₄ coated aluminum plates; the spots were visualized by UV light or iodine chamber. UV-Vis absorption spectra were recorded with a Jasco V-560 spectrophotometer. Compound nomenclatures were generated with ChemBioDraw Ultra version 16.0.0.82.

General procedure for the synthesis of compounds 5–8

To a solution of the appropriate halomethyl acid derivative (2.93 mmol) in CH₃CN, AgNO₃ (11.72 mmol, 1.99 g) was added, and the reaction mixture was stirred at rt in the dark. The precipitate (silver halide) was filtered off, and the residue triturated. The solvent was evaporated, and the product used as is without any further purification.

4-((nitrooxy)methyl)benzoic acid (**5**)

The compound has been prepared using 4-(chloromethyl)benzoic acid (2.93 mmol, 0.50 g). Stirring was continued over 4 h at rt in the dark. The AgCl precipitate was filtered off, and the solvent evaporated. The crude product was triturated with CHCl₃ (10 mL) and filtered to remove the unreacted AgNO₃ and AgCl. Yield: 80%, white solid. ¹H NMR (200 MHz, CDCl₃) δ 8.09 (d, *J* = 8.1 Hz, 2H), 7.53 (d, *J* = 8.2 Hz, 2H), 5.51 (s, 2H).

3-((nitrooxy)methyl)benzoic acid (**6**)

The compound has been prepared using 3-(chloromethyl)benzoic acid (2.93 mmol, 0.50 g). Stirring was continued over 4 h at rt in the dark. The AgCl precipitate was filtered, and the solvent evaporated. The crude product was triturated with CHCl₃ (10 mL) and filtered to remove the unreacted AgNO₃ and AgCl. Yield: 76%, white solid. ¹H NMR (200 MHz, CDCl₃) δ 8.14–8.17 (m, 2H), 7.67 (d, *J* = 7.8 Hz, 1H), 7.49–7.58 (m, 1H), 5.49 (s, 2H).

2-(4-((nitrooxy)methyl)phenyl)acetic acid (**7**)

The compound has been prepared using 2-(4-(bromomethyl)phenyl)acetic acid (1.96 mmol, 0.45 g) and the reaction mixture was stirred at rt in the dark for 2 days. The AgBr precipitate was filtered off, and the residue triturated with brine and extracted with EtOAc. Yield: 75%, white solid. ¹H NMR (200 MHz, CDCl₃) δ 7.29–7.44 (m, 4H), 5.42 (s, 2H), 3.68 (s, 2H).

2-(3-((nitrooxy)methyl)phenyl)acetic acid (**8**)

The compound has been prepared using 2-(3-(bromomethyl)phenyl)acetic acid (1.96 mmol, 0.45 g) and the reaction mixture was stirred at rt in the dark for 2 days. The AgBr precipitate was filtered off, and the residue triturated with brine and extracted with EtOAc. Yield: 70%, white solid. ¹H NMR (200 MHz, CDCl₃) δ 6.76–8.02 (m, 4H), 5.42 (s, 2H), 3.68 (s, 2H).

General procedure for the synthesis of compounds 9–20

To a solution of the appropriate nitrooxy-substituted benzoic acid derivative **5–8** (1.01 mmol) in CH₃CN (5 mL), HOBT (1.53 mmol, 0.21 g), and EDC (1.52 mmol, 0.29 g) were added. After stirring for 20 min, the appropriate substituted amine (2.02 mmol) has been added and the resulting mixture was stirred at rt for 5 h. After the reaction was complete, the solvent was evaporated to dryness and the crude solubilized in CH₂Cl₂ (20 mL), washed with H₂O (2 x 10 mL), and brine (5 mL), and dried under anhydrous Na₂SO₄. The solvent was removed under vacuum and the residue was purified via silica gel chromatography (10% MeOH in EtOAc and then 10% MeOH + 3% NH₄OH in EtOAc) to provide the desired product.

3-((2-(4-benzylpiperidin-1-yl)ethyl)carbamoyl)benzyl nitrate (**9**)

The compound has been prepared using 3-((nitrooxy)methyl)benzoic acid (1.01 mmol, 0.20 g) and 4-(4-benzylpiperidin-1-yl)butan-1-amine (2.02 mmol, 0.44 g). Yield: 73%, white solid. ¹H NMR (200 MHz, CDCl₃) δ 7.92 (ddd, *J* = 0.98, 2.83, 5.56 Hz, 2H), 7.78 (dd, *J* = 1.56, 7.42 Hz, 1H), 7.19–7.50 (m, 6H), 7.10 (br. s, 1H), 5.53 (s, 2H), 3.51 (d, *J* = 5.85 Hz, 2H), 2.93 (d, *J* = 11.71 Hz, 2H), 2.45–2.61 (m, 7H), 1.95–2.01 (m, 2H), 1.60–1.69 (m, 2H). ¹³C NMR (200 MHz, CDCl₃) δ 166.41, 143.23, 140.41, 136.10, 129.86, 129.04, 128.15, 127.45, 125.84, 124.56, 120.08, 81.60, 56.46, 53.58, 43.05, 37.83, 36.45, 32.13. Anal. calcd for C₂₂H₂₇N₃O₄: C, 66.48; H, 6.85; N, 10.57; O, 16.10. Found: C, 66.35; H, 6.86; N, 10.59; O, 16.14.

3-((3-(4-benzylpiperidin-1-yl)propyl)carbamoyl)benzyl nitrate (**10**)

The compound has been prepared using 3-((nitrooxy)methyl)benzoic acid (1.01 mmol, 0.20 g) and 3-(4-benzylpiperidin-1-yl)propan-1-amine (2.02 mmol, 0.47 g). Yield: 70%, white solid. ¹H NMR (200 MHz, CDCl₃) δ 8.60 (br. s, 1H), 7.91–8.10 (m, 3H), 7.16–7.42 (m, 6H), 5.56 (s, 2H), 3.50–3.71 (m, 4H), 2.96–3.12 (m, 2H), 2.63 (d, *J* = 6.64 Hz, 2H), 2.20 (d, *J* = 5.85 Hz, 2H), 1.71–2.02 (m, 4H), 1.19–1.33 (m, 1H). ¹³C NMR (200 MHz, CDCl₃) δ 166.91, 138.80, 136.32, 134.61, 129.79, 128.90, 128.52, 127.96, 126.45, 124.58, 120.02, 81.67, 40.39, 36.92, 36.26, 23.24, 22.67, 17.59. Anal. calcd for C₂₃H₂₉N₃O₄: C, 67.13; H, 7.10; N, 10.21; O, 15.55. Found: C, 66.97; H, 7.08; N, 10.23; O, 15.57.

3-((4-(4-benzylpiperidin-1-yl)butyl)carbamoyl)benzyl nitrate (**11**)

The compound has been prepared using 3-((nitrooxy)methyl)benzoic acid (1.01 mmol, 0.20 g) and 4-(4-benzylpiperidin-1-yl)butan-1-amine (2.02 mmol, 0.50 g). Yield: 75%, white solid. ¹H NMR (200 MHz, CDCl₃) δ 7.97 (dd, *J* = 0.98, 8.00 Hz, 1H), 7.72–7.88 (m, 2H), 7.16–7.55 (m, 6H), 6.97 (br. s, 1H), 5.58 (s, 2H), 2.89 (d, *J* = 11.32 Hz, 2H), 2.47 (d, *J* = 6.64 Hz, 2H), 2.34 (t, *J* = 6.44 Hz, 2H), 1.84 (t, *J* = 11.71 Hz, 3H), 1.50–1.72 (m, 7H), 1.09–1.35 (m, 3H). ¹³C NMR 166.85, 140.46, 135.70, 133.38, 132.36, 128.99, 128.09, 125.73, 124.58, 119.96, 108.60, 81.88, 58.16, 53.80, 43.02, 39.90, 37.74, 31.84, 27.33, 24.49. Anal. calcd for C₂₄H₃₁N₃O₄: C, 67.74; H, 7.34; N, 9.88; O, 15.04. Found: C, 67.61; H, 7.35; N, 9.86; O, 15.06.

3-((5-(4-benzylpiperidin-1-yl)pentyl)carbamoyl)benzyl nitrate (**12**)

The compound has been prepared using 3-((nitrooxy)methyl)benzoic acid (1.01 mmol, 0.20 g) and 5-(4-benzylpiperidin-1-yl)pentan-1-amine (2.02 mmol, 0.53 g). Yield: 79%, white solid, ¹H NMR (500 MHz, CDCl₃) δ 7.97 (d, *J* = 8.31 Hz, 1H), 7.36–7.41 (m, 1H), 7.30–7.35 (m, 1H), 7.24–7.29 (m, 3H), 7.16–7.20 (m, 1H), 7.13 (d, *J* = 7.34 Hz, 2H), 6.19 (br. s, 1H), 5.58 (s, 2H), 3.40–3.46 (m, 2H), 2.89 (d, *J* = 11.74 Hz, 2H), 2.53 (d, *J* = 6.85 Hz, 2H), 2.27–2.33 (m, 2H), 1.80–1.88 (m, 2H), 1.59–1.67 (m, 4H), 1.46–1.58 (m, 3H), 1.23–1.44 (m, 4H). ¹³C NMR (500 MHz, CDCl₃) δ 166.66, 143.15, 140.44, 135.36, 132.43, 129.00, 128.08, 125.72, 124.59, 119.92, 81.86, 58.56,

53.58, 42.96, 39.88, 37.71, 31.66, 29.22, 26.24, 24.79. Anal. calcd for $C_{25}H_{33}N_3O_4$: C, 68.31; H, 7.57; N, 9.56; O, 14.56. Found: C, 68.44; H, 7.56; N, 9.54; O, 14.59.

4-((2-(4-benzylpiperidin-1-yl)ethyl)carbamoyl)benzyl nitrate (**13**)

The compound has been prepared using 4-((nitrooxy)methyl)benzoic acid (1.01 mmol, 0.20 g) and 4-(4-benzylpiperidin-1-yl)butan-1-amine (2.02 mmol, 0.44 g). Yield: 75%, white solid. 1H NMR (500 MHz, $CDCl_3$) δ 7.77 (d, $J = 7.8$ Hz, 2H), 7.48 (d, $J = 8.3$ Hz, 2H), 7.25–7.42 (m, 5H), 7.01 (br. s., 1H), 5.59 (s, 2H), 3.52 (q, $J = 5.7$ Hz, 2H), 2.92 (d, $J = 11.2$ Hz, 2H), 2.54–2.62 (m, 4H), 1.96–2.04 (m, 2H), 1.68 (d, $J = 13.2$ Hz, 2H), 1.57 (ddt, $J = 14.9, 7.5, 3.7$ Hz, 1H), 1.24–1.35 (m, 2H). ^{13}C NMR (200 MHz, $CDCl_3$) δ 166.43, 143.25, 140.43, 136.12, 129.88, 128.17, 127.68, 125.84, 120.08, 81.60, 56.46, 53.58, 43.05, 37.83, 36.45, 32.13. Anal. calcd for $C_{22}H_{27}N_3O_4$: C, 66.48; H, 6.85; N, 10.57; O, 16.10. Found: C, 66.31; H, 6.86; N, 10.59; O, 16.06.

4-((3-(4-benzylpiperidin-1-yl)propyl)carbamoyl)benzyl nitrate (**14**)

The compound has been prepared using 4-((nitrooxy)methyl)benzoic acid (1.01 mmol, 0.20 g) and 3-(4-benzylpiperidin-1-yl)propan-1-amine (2.02 mmol, 0.47 g). Yield: 70%, white solid. 1H NMR (500 MHz, $CDCl_3$) δ 8.53 (br. s., 1H), 7.27–7.41 (m, 5H), 7.25 (d, $J = 7.2$ Hz, 2H), 7.07 (d, $J = 6.8$ Hz, 2H), 5.61 (s, 2H), 3.53–3.61 (m, 2H), 3.01 (d, $J = 11.7$ Hz, 2H), 2.53–2.58 (m, 2H), 2.49 (d, $J = 7.3$ Hz, 2H), 1.92 (t, $J = 11.5$ Hz, 2H), 1.80 (dt, $J = 11.7, 5.9$ Hz, 4H), 1.67 (d, $J = 12.2$ Hz, 2H), 1.56 ppm (ddt, $J = 15.0, 7.4, 3.7$ Hz, 1H). ^{13}C NMR (200 MHz, $CDCl_3$) δ 166.46, 145.17, 143.25, 140.18, 132.40, 128.94, 128.20, 125.88, 124.53, 81.98, 58.5, 54.0, 43.1, 41.0, 38.80, 32.1, 24.08. Anal. calcd for $C_{23}H_{29}N_3O_4$: C, 67.13; H, 7.10; N, 10.21; O, 15.55. Found: C, 66.86; H, 7.04; N, 10.24; O, 15.58.

4-((4-(4-benzylpiperidin-1-yl)butyl)carbamoyl)benzyl nitrate (**15**)

The compound has been prepared using 4-((nitrooxy)methyl)benzoic acid (1.01 mmol, 0.20 g) and 4-(4-benzylpiperidin-1-yl)butan-1-amine (2.02 mmol, 0.50 g). Yield: 80%, white solid. 1H NMR (200 MHz, $CDCl_3$) δ 7.75 (d, $J = 8.20$ Hz, 2H), 7.46 (d, $J = 7.81$ Hz, 2H), 7.07–7.40 (m, 5H), 6.98 (br. s., 1H), 5.59 (s, 2H), 3.37–3.54 (m, 2H), 2.81–3.00 (m, 2H), 2.48 (d, $J = 6.64$ Hz, 2H), 2.36 (t, $J = 6.64$ Hz, 2H), 1.85 (t, $J = 10.93$ Hz, 2H), 1.40–1.74 (m, 7H), 1.09–1.34 (m, 2H). ^{13}C NMR (200 MHz, $CDCl_3$) δ 166.88, 142.42, 136.22, 133.83, 129.85, 129.04, 128.18, 127.57, 124.59, 81.63, 65.76, 53.80, 49.78, 42.36, 38.24, 37.68, 31.74, 26.10. Anal. calcd for $C_{24}H_{31}N_3O_4$: C, 67.74; H, 7.34; N, 9.88; O, 15.04. Found: C, 67.89; H, 7.36; N, 9.85; O, 15.06.

4-((5-(4-benzylpiperidin-1-yl)pentyl)carbamoyl)benzyl nitrate (**16**)

The compound has been prepared using 4-((nitrooxy)methyl)benzoic acid (1.01 mmol, 0.20 g) and 5-(4-benzylpiperidin-1-yl)pentan-1-amine (2.02 mmol, 0.53 g). Yield: 83%, white solid. 1H NMR (500 MHz, $CDCl_3$) δ 7.77 (d, $J = 7.83$ Hz, 1H), 7.50 (d, $J = 7.83$ Hz, 1H), 7.39–7.43 (m, 1H), 7.30–7.34 (m, 1H), 7.24–7.29 (m, 3H), 7.12 (d, $J = 6.85$ Hz, 2H), 6.23 (br. s., 1H), 5.57 (s, 2H), 3.43 (q, $J = 6.85$ Hz, 2H), 2.92–2.97 (m, 2H), 2.52 (d, $J = 7.34$ Hz, 2H), 2.33–2.38 (m, 2H), 1.80 (t, $J = 11.25$ Hz, 2H), 1.49–1.68 (m, 7H), 1.32–1.44 (m, 4H). ^{13}C NMR (200 MHz, $CDCl_3$) 166.63, 140.60, 136.18, 135.93, 129.88, 129.07, 128.12, 127.37, 125.76, 81.54, 58.76, 53.93, 43.13, 39.98, 37.87, 31.97, 29.42, 26.55, 24.93. Anal. calcd for $C_{25}H_{33}N_3O_4$: C, 68.31; H, 7.57; N, 9.56; O, 14.56. Found: C, 68.3; H, 7.55; N, 9.58; O, 14.59.

3-((1-benzylpiperidin-4-yl)carbamoyl)benzyl nitrate (**17**)

The compound has been prepared using 3-((nitrooxy)methyl)benzoic acid (1.01 mmol, 0.20 g) and 4-amino-benzylpiperidine (2.02 mmol, 0.38 g). Yield: 79%, white solid. 1H NMR (200 MHz, $CDCl_3$) δ 7.97 (dd, $J = 1.76, 7.22$ Hz, 1H), 7.68–7.80 (m, 2H), 7.21–7.88 (m, 6H), 5.90 (d, $J = 7.81$ Hz, 1H), 5.57 (s, 2H), 3.87–4.11 (m, 3H), 3.53 (s,

2H), 2.87 (d, $J = 12.10$ Hz, 2H), 2.17 (t, $J = 11.51$ Hz, 2H), 2.00 (d, $J = 11.71$ Hz, 2H), 1.45–1.68 (m, 2H). ^{13}C NMR (200 MHz, CDCl_3) δ 165.99, 143.26, 138.19, 135.47, 129.12, 128.25, 127.10, 124.63, 81.86, 63.02, 52.27, 47.24, 32.21. Anal. calcd for $\text{C}_{20}\text{H}_{23}\text{N}_3\text{O}_4$: C, 65.03; H, 6.28; N, 11.37; O, 17.32. Found: C, 65.16; H, 6.29; N, 11.34; O, 17.35.

3-(2-((1-benzylpiperidin-4-yl)amino)-2-oxoethyl)benzyl nitrate (**18**)

The compound has been prepared using 2-(3-((nitrooxy)methyl)phenyl)acetic acid (1.01 mmol, 0.21 g) and 4-amino-benzylpiperidine (2.02 mmol, 0.38 g). Yield: 81%, white solid. ^1H NMR (200 MHz, CDCl_3) δ 7.18–7.45 (m, 9H), 5.50 (s, 2H), 3.64–3.89 (m, 1H), 3.45 (s, 2H), 2.75 (d, $J = 11.71$ Hz, 2H), 1.98–2.17 (m, 2H), 1.83 (d, $J = 12.10$ Hz, 2H), 1.23–1.49 (m, 2H). ^{13}C NMR (200 MHz, CDCl_3) δ 169.51, 143.23, 138.30, 136.74, 130.52, 129.75, 129.03, 127.02, 124.50, 120.08, 81.97, 62.96, 52.11, 46.60, 43.54, 32.02. Anal. calcd for $\text{C}_{21}\text{H}_{25}\text{N}_3\text{O}_4$: C, 65.78; H, 6.57; N, 10.96; O, 16.69. Found: C, 65.94; H, 6.58; N, 10.92; O, 16.74.

4-((1-benzylpiperidin-4-yl)carbamoyl)benzyl nitrate (**19**)

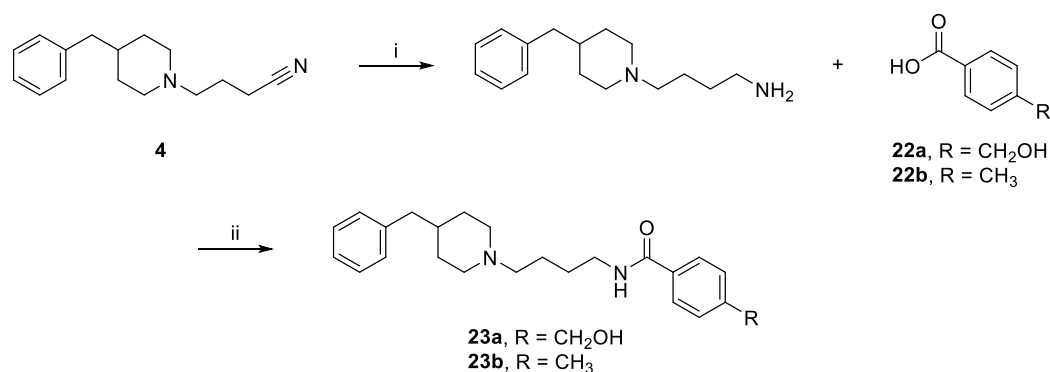
The compound has been prepared using 3-((nitrooxy)methyl)benzoic acid (1.01 mmol, 0.20 g) and 4-amino-benzylpiperidine (2.02 mmol, 0.38 g). Yield: 75%, white solid. ^1H NMR (200 MHz, CDCl_3) δ 7.72 (d, $J = 8.31$ Hz, 2H), 7.45 (d, $J = 8.20$ Hz, 2H), 7.22–7.41 (m, 5H), 5.97 (d, $J = 7.81$ Hz, 1H), 5.58 (s, 2H), 3.88–4.16 (m, 1H), 3.52 (s, 2H), 2.86 (d, $J = 12.49$ Hz, 2H), 2.17 (t, $J = 11.71$ Hz, 2H), 2.02 (d, $J = 12.49$ Hz, 2H), 1.45–1.67 (m, 2H). ^{13}C NMR (200 MHz, CDCl_3) δ 165.98, 143.27, 138.07, 129.90, 129.14, 128.26, 127.37, 124.60, 81.50, 63.02, 52.25, 47.18, 32.20. Anal. calcd for $\text{C}_{20}\text{H}_{23}\text{N}_3\text{O}_4$: C, 65.03; H, 6.28; N, 11.37; O, 17.32. Found: C, 64.88; H, 6.26; N, 11.39; O, 17.27.

4-(2-((1-benzylpiperidin-4-yl)amino)-2-oxoethyl)benzyl nitrate (**20**)

The compound has been prepared using 4-((nitrooxy)methyl)phenylacetic acid (1.01 mmol, 0.21 g) and 4-amino-benzylpiperidine (2.02 mmol, 0.38 g). Yield: 79%, white solid. ^1H NMR (200 MHz, CDCl_3) δ 7.92–8.01 (m, 1H), 7.18–7.45 (m, 8H), 5.53 (s, 2H), 5.15 (d, $J = 8.20$ Hz, 1H), 3.66–3.89 (m, 1H), 3.42–3.56 (m, 4H), 2.75 (d, $J = 12.10$ Hz, 2H), 2.07 (dt, $J = 2.54, 11.61$ Hz, 2H), 1.80 (d, $J = 12.10$ Hz, 2H), 1.17–1.40 (m, 2H). ^{13}C NMR (200 MHz, CDCl_3) δ 169.53, 138.33, 136.76, 132.11, 130.52, 129.75, 129.03, 128.20, 127.89, 81.97, 62.98, 52.13, 46.62, 43.56, 32.04. Anal. calcd for $\text{C}_{21}\text{H}_{25}\text{N}_3\text{O}_4$: C, 65.78; H, 6.57; N, 10.96; O, 16.69. Found: C, 65.94; H, 6.55; N, 10.98; O, 16.71.

General procedure for the synthesis of compounds 23a and 23b

Scheme S1. Synthetic strategy for the preparation of compounds 23a and 23b



Reagents and conditions: (i) LiAlH₄, THF, rt, N₂; (ii) EDC, HOBT, CH₃CN, rt, on.

To a solution of the appropriate benzoic acid derivative **22a** or **22b** (0.46 mmol) in CH₃CN (5 mL), HOBT (0.69 mmol, 0.09 g), and EDC (0.69 mmol, 0.13 g) were added. After stirring for 20 min, appropriate amine (0.92 mmol, 226 mg) has been added, and the resulting mixture was stirred at rt overnight. After the reaction was complete, the solvent was evaporated to dryness and the crude dissolved in CH₂Cl₂ (20 mL), washed with H₂O (2 x 10 mL), brine (5 mL), and dried under anhydrous Na₂SO₄. The solvent was removed under vacuum, and the residue was purified via silica gel chromatography (10% MeOH in EtOAc) to provide the desired product.

N-(4-(4-benzylpiperidin-1-yl)butyl)-4-(hydroxymethyl)benzamide (**23a**)

The compound has been prepared using 4-(hydroxymethyl)benzoic acid (**a**, 0.46 mmol, 0.07 g). Yield: 49%, white solid. ¹H NMR (200 MHz, CDCl₃) δ 8.13 (br. s., 1H), 7.87 (d, *J*=7.4 Hz, 2H), 7.17–7.36 (m, 5H), 7.10 (d, *J*=7.8 Hz, 2H), 4.63 (br. s., 2H), 3.28–3.62 (m, 4H), 2.91 (br. s., 2H), 2.45–2.74 (m, 4H), 1.51–1.97 (m, 8H), 1.21 (t, *J*=7.0 Hz, 2H). ¹³C NMR (200 MHz, CDCl₃) δ 167.79, 145.22, 138.98, 132.49, 129.32, 123.09, 65.82, 57.67, 42.58, 34.81, 26.16. Anal. calcd for C₂₄H₃₂N₂O₂: C, 75.75; H, 8.48; N, 7.36; O, 8.41. Found: C, 75.91; H, 8.43; N, 7.35; O, 8.44.

N-(4-(4-benzylpiperidin-1-yl)butyl)-4-methylbenzamide (**23b**)

The compound has been prepared using 4-methylbenzoic acid (**b**, 0.44 mmol, 0.06 g). Yield: 60%, white solid. ¹H NMR (200 MHz, CDCl₃) δ 7.88 (d, *J*=8.2 Hz, 2H), 7.61 (t, *J*=5.9 Hz, 1H), 7.20–7.39 (m, 5H), 7.10–7.19 (m, 2H), 3.39–3.60 (m, 4H), 2.91–3.04 (m, 2H), 2.48–2.69 (m, 4H), 2.41 (s, 3H), 1.66–2.06 (m, 9H). ¹³C NMR (200 MHz, CDCl₃) δ 167.60, 141.64, 138.92, 131.17, 129.02, 128.88, 128.43, 127.26, 126.33, 52.68, 41.79, 37.73, 28.81, 26.10, 20.75. Anal. calcd for C₂₄H₃₂N₂O: C, 79.08; H, 8.85; N, 7.68; O, 4.39. Found: C, 79.21; H, 8.81; N, 7.65; O, 4.40.

Computational procedures

Molecular docking

Flexible ligands docking experiments were performed employing AutoDock 4.2.6 software implemented in YASARA (v. 19.5.5, YASARA Biosciences GmbH, Vienna, Austria)^{1, 2} using the crystal structure of the human σ₁ receptor model bound to PD144418 (PDB 5HK1) retrieved from the PDB_REDO Data Bank as a fully optimized one, and the Lamarckian genetic algorithm (LGA). The maps were generated by the program AutoGrid (4.2.6) with a spacing of 0.375 Å and dimensions that encompass all atoms extending 5 Å from the surface of the structure of the crystallized ligands. All the parameters were inserted at their default settings as previously reported [30]. In the docking tab, the

macromolecule and ligand are selected, and GA parameters set as $ga_runs = 100$, $ga_pop_size = 150$, $ga_num_evals = 25000000$, $ga_num_generations = 27000$, $ga_elitism = 1$, $ga_mutation_rate = 0.02$, $ga_crossover_rate = 0.8$, $ga_crossover_mode = two\ points$, $ga_cauchy_alpha = 0.0$, $ga_cauchy_beta = 1.0$, number of generations for picking worst individual = 10. Since no water molecules are directly involved in complex stabilization, they were not considered in the docking process. All protein amino acid residues were kept rigid whereas all single bonds of ligands were treated as fully flexible. Docking for the σ_2 receptor was performed using the homology model of the σ_2 receptor previously built by the same authors maintaining the same parameters as described above.³

Table S1. Calculated Binding Energies (kcal/mol) and Binding Constants K_i (nM) for the Binding Sites of σ_1 and σ_2 Receptors for Compounds 9-20

Compound	Calcd ΔG_{σ_1}	Calcd $K_{i\sigma_1}$	Exp $K_{i\sigma_1}$	Calcd ΔG_{σ_2}	Calcd $K_{i\sigma_2}$	Exp $K_{i\sigma_2}$
9	-9.96	49.61	49	-8.81	345.91	330
10	-9.83	61.79	64	-9.68	79.60	93
11	-9.20	179.20	148	-9.49	109.71	75
12	-10.27	29.39	50	-9.19	182.08	142
13	-9.77	68.38	89	-7.58	2760.6	2673
14	-9.13	201.50	145	-8.89	302.20	230
15	-9.03	238.57	250	-9.33	143.75	89
16	-10.18	34.22	93	-9.69	78.30	70
17	-10.34	26.11	24	-11.74	2.46	19
18	-11.23	5.81	19	-8.75	382.79	320
19	-10.73	13.52	22	-9.03	238.57	270
20	-9.14	198.13	170	-7.68	2331.71	2514
Haloperidol	-10.9	10.14	2.5	-10.34	30.92	16

Docked poses analysis in σ_2 receptor

Compounds with similar aliphatic linker length in the series (**11** and **16**) show interactions comparable with that observed in the σ_1 receptor pocket. In fact, compound **16**, the most active of the **9–16** series ($K_{i\sigma_2}$ of 70 nM) forms a salt bridge with the Asp29 residue utilizing the pyridinium proton and a hydrogen bond with the Asp56, while the benzyl portion in position 4 to the piperidine ring shows hydrophobic interactions with the residues Val33, Leu26, Leu78, and π - π interaction with Pro79 (Figure S2).

The good affinity of compound **17** with the σ_2 receptor ($K_{i\sigma_2}$ of 19 nM) is due to both the double hydrogen bond and the cation- π interaction between receptor and ligand. In fact, the pyridinium proton forms a salt bridge with Asp29 while the amidic hydrogen forms a hydrogen bond with Asp56; the nitrate group is stabilized by the cation- π interaction with the Phe71 and Pro113 residues (Figure S2)

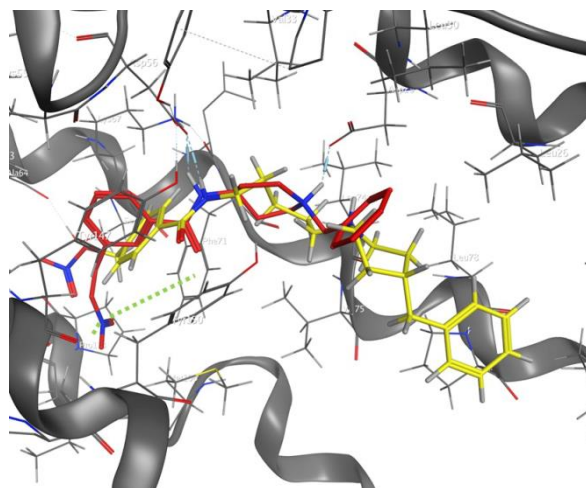


Figure S1. 3D-structures of **16** (yellow) and **17** (red) bound to the σ_2 receptor, showing the salt bridge and the cation- π (green dotted line) interactions, and the hydrogen bonds with Asp29 and Asp56 (blue dotted line).

Molecular optimization

The semi-empirical calculations were performed using the parameterized model number 6 Hamiltonian⁴ as implemented in MOPAC package⁵ (MOPAC2016 v. 18.151, Stewart Computational Chemistry, Colorado Springs, Colorado, USA).

Molecular dynamics simulations

The MD simulations of the mature human σ_1 receptor/ligand were performed with the YASARA Structure package (19.11.5).¹ A periodic simulation cell with boundaries extending 8 Å from the surface of the complex was employed. The box was filled with water molecules, with a maximum sum of all bumps water of 1.0 Å, and a density of 0.997 g/mL. YASARA's pK_a utility used to assign pK_a values at pH 7.4⁶, and system charges was neutralized with NaCl (0.9% by mass). Water molecules were deleted to readjust the solvent density to 0.997 g/mL. The final system dimensions were approximately 70 × 70 × 90 Å³. The ligand force field parameters were generated with the AutoSMILES utility, employs semiempirical AM1 geometry optimization. Moreover, the assignment of charges, by the assignment of the AM1BCC atom and bond types with refinement using the RESP charges, and finally the assignments of general AMBER force field atom types. Optimization of the hydrogen bonds network of the various enzyme-ligand complexes was obtained using the method established by Hooft et al.⁷ This model allowed us to address ambiguities arising from multiple side-chain conformations and protonation states that are not well resolved in the electron density. Short MD simulation was run on the solvent only. The entire system was then energy minimized using first a steepest descent minimization to remove conformational stress, followed by a simulated annealing minimization until convergence (<0.01 kcal/mol Å). The MD simulation was then initiated, using the NPT ensemble at 298 K, and integration time steps for intramolecular and intermolecular forces every 1.25 fs and 2.5 fs, respectively. Finally, short 10 ns MD simulations were conducted for the assessment of the correct pose, and a final MD simulation of 100 ns was performed. The conformations of each system were recorded every 100 ps.

Molecular dynamics simulations study and trajectories analysis of compound 18

Before executing the 100 ns MD simulation, it was performed a short MD one (10 ns) to identify the most stable pose. As shown in Figure S2a, compound **18** shows a bidentate interaction between the piperidinium proton (due to the formation of the salt bridge) and the amidic hydrogen with the Glu172 residue.

The ligand is placed inside the pocket, orienting the benzyl group along the bottom side of the receptor and the nitrate group toward the upper. After 100 ns of MD simulation, it is interesting to note that the ligand maintains the

salt bridge with the Glu172 residue, and a new hydrogen bond bridge is established, favored by a water molecule between the Glu172 and Asp126 residues and the amidic hydrogen.

Furthermore, the His154 residue maintains a cation- π interaction with the nitrate group, further stabilizing the laying of the ligand inside the receptor. After 100 ns of MD simulation, the distance between the nitrate group and the residue His154 decreases by 0.49 Å (from 3.80 Å to 3.31 Å) while the distance between the pyridinium and Glu172 proton decreases by 0.88 Å (from 2.56 Å to 1.68 Å) (Figure S2b). The redocking of compound **18**, using the pose after 100 ns MD simulation, resulted in a calculated K_i value of 15 nM, which is in excellent agreement with the experimental one (19 nM).

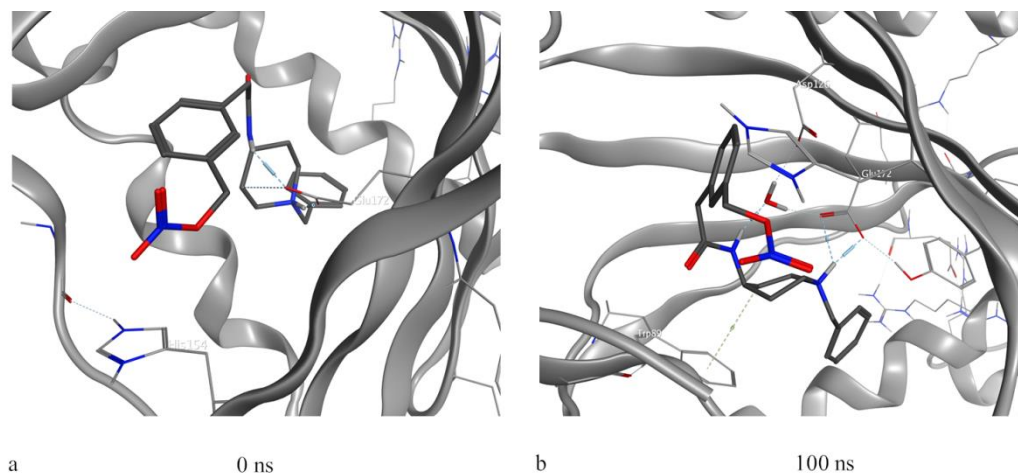


Figure S2. Poses of compound **18** bound to the σ_1 receptor at 0 ns (a) and 100 ns (b) of MD simulation, showing salt bridge interaction with Glu172 (blue dotted line) and extensive hydrophobic contacts with other binding pocket residues.

The overall RMSD for the protein system appeared to have reached equilibrium after 13 ns with slight inflation at 36 ns, while the stabilization of the ligand after 8 ns. The binding energy of the ligand undergoes a slight increase after 58 ns, remaining overall stable throughout the MD simulation. (Figure S3).

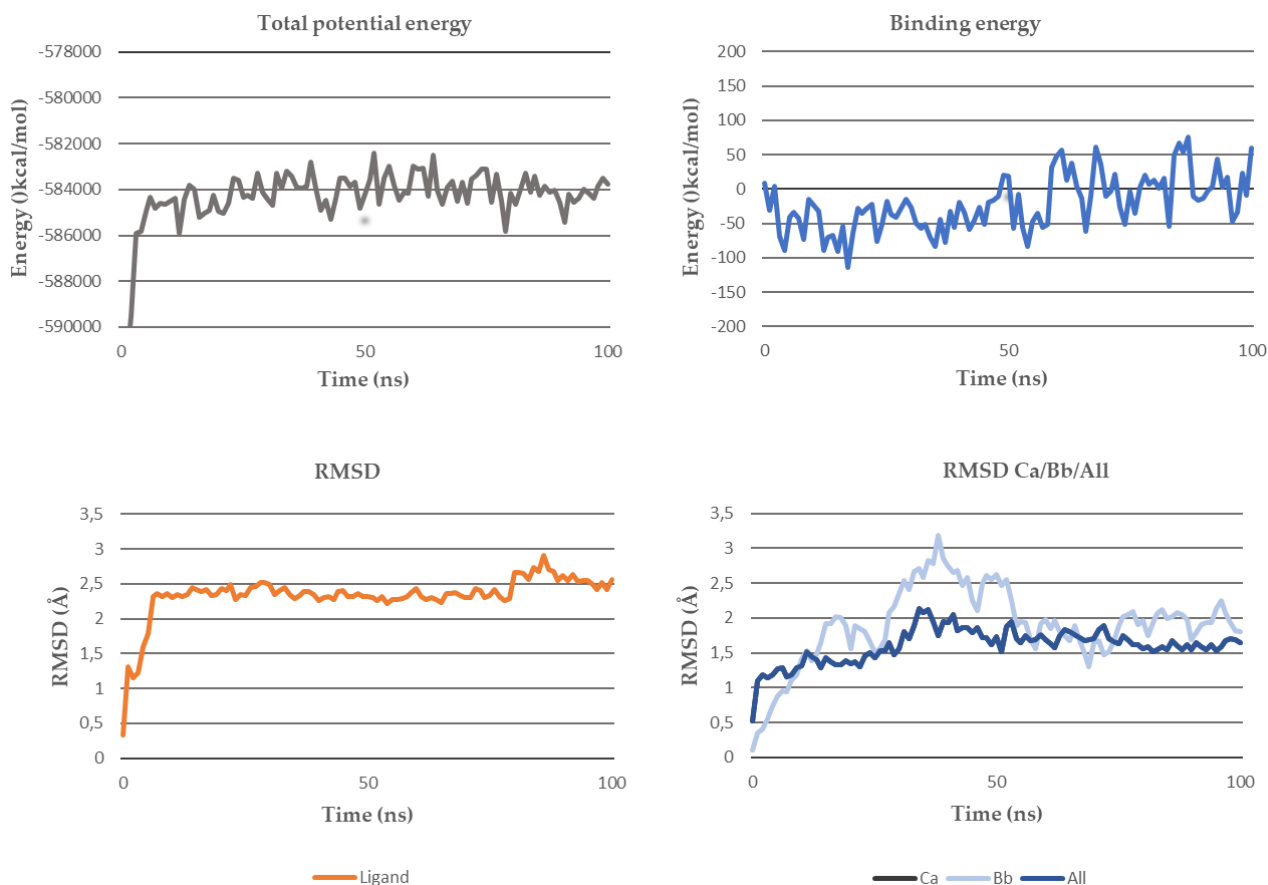


Figure S3. Total potential energy of the system (up-left), binding energy of the ligand (up-right), RMSD ligand after superposition on the receptor (down-left), and RMSDs from the starting protein structure (down-right) of σ_2 receptor and its complex with compound **18**.

Biological evaluation

Radioligand binding assays

In vitro σ_1 ligand binding assays were carried out in Tris-HCl buffer (50 mmol/L, pH 7.4) for 150 min at 37 °C by incubating the guinea pig brain membrane homogenates (500 $\mu\text{g}/\text{sample}$) with [^3H]-(+)-pentazocine (3 nM) and increasing concentrations (from 10^{-5} to 10^{-11} M) of the tested compound in a final volume of 1 mL. Haloperidol (10 μM) was employed to measure non-specific binding. Bound and free radioligand were divided by fast filtration under reduced pressure using a Millipore filter apparatus through Whatman GF/B glass fiber filters, which were presoaked for 1 h in a 0.5% poly(ethyleneimine) solution. Filters were washed with the same ice-cold buffer (2×4 mL), air-dried, and then soaked in 4 mL of Ultima Gold MV Scintillation cocktail. The amount of bound radioactivity on the filters was measured using a liquid scintillation counter Beckman LS6500.⁸

For in vitro σ_2 binding assays, the membranes (360 $\mu\text{g}/\text{sample}$) were incubated with 3 nM [^3H]-1,3-di-o-tolylguanidine ([^3H]-DTG) in the presence of the σ_1 masking agent (+)-SKF10,047 (400 nM) at rt for 120 min in 0.5 mL final volume of binding buffer (50 mmol/L Tris-HCl, pH 8.0). Non-specific binding was evaluated with unlabeled DTG (5 μM). Assays were terminated by adding ice-cold 10 mM Tris-HCl washing buffer (pH 8.0), and each sample was filtered through Whatman GF/B glass fiber filters, presoaked for 1 h in a 0.5% poly(ethyleneimine) solution. Then, filters were washed with ice-cold buffer (2×4 mL), and the amount of bound radioactivity was

determined by liquid scintillation counting as described above.⁹ Results are expressed as inhibition constants (K_i values) and calculated using GraphPad Prism (GraphPad Software, San Diego, CA, USA).

Detection of Nitrite: Griess Reaction

The method is based on the reaction of diazocoupling of nitrite with the Griess reagent.¹⁰ A 10 mM solution of the appropriate compound in DMSO was diluted with Tris-HCl (50 mM, pH 7.4). The final concentration of the compounds was 100 μ M. After incubation for 30 min at 37 °C, 500 μ L of each compound were incubated for 30 min at 25° C in phosphate buffer (50 mM pH 7.4) with NADPH (50 μ M) and nitrate reductase (60 mU). To remove the excess of NADPH, which could interfere with the Griess reagent, samples were then treated with pyruvate (5 mM) and lactic dehydrogenase (1U). After 10 minutes, 500 μ l of Griess reagent was added to the reaction mixture. After 10 min at rt, the absorbance was measured spectrophotometrically at $\lambda=540$ nm; calibration was obtained using known amounts of KNO_2 (0.1 to 20 μ M). The yields of nitrite are expressed as NO_2^- (μ M); the experiments were performed in triplicate. Data are expressed as the mean \pm SD.¹¹

Cell culture

The human epithelial colorectal adenocarcinoma cell line (CaCo-2) was provided by ATCC cell bank (Rockville, MD, USA), and routinely maintained in DMEM (Gibco BRL, Life Technologies) supplemented with 10% fetal calf serum, 1% sodium pyruvate, 1% L-glutamine solution, and 1% streptomycin/penicillin. The human breast adenocarcinoma cell line (MCF-7) was obtained from the American Type Culture Collection (Rockville, MD, USA) and maintained in Dulbecco's modified Eagle's medium (DMEM) containing 10% fetal calf serum, 100 U/mL penicillin, and 100 μ g/mL streptomycin (Sigma–Aldrich, Italy). The human immortalized cell lines of dermal fibroblasts (HFF-1) provided by ATCC (Manassas, VA, USA) were suspended in Dulbecco's modified essential medium (GIBCO BRL, Life Technologies) supplemented with 10% heat-inactivated fetal calf serum, 1.0 mM sodium pyruvate, 2.0 mM l-glutamine, streptomycin (50 μ g/mL) and penicillin (50 U/mL). Cell lines were cultured in a humidified atmosphere of 5% CO_2 /95% air at 37 °C. Cells from semi-confluent cultures were detached using 0.5% trypsin/0.2% EDTA and seeded in complete medium. Individual wells of a 96-well tissue culture microtiter plate (Falcon; Becton-Dickinson) were seeded with complete media containing cells in exponential growth at an initial density of 10×10^3 cells per flat-bottomed well (200 μ L per microwell). The plates were incubated at 37 °C in a humidified 5% CO_2 incubator for 24 h before the experiments. The cells were treated for 24 h with different concentrations (5, 10, 25, 35, 50, 75, or 100 μ M) of the compound solutions previously dissolved in the minimum amount of DMSO and diluted with the medium; the plates were incubated at 37 °C.

Cell viability

Cell viability was assessed by 3-(4,5-dimethylthiazol-2-yl)-2,5-diphenyltetrazolium bromide (MTT) assay, which is based on the conversion of a substrate containing a tetrazolium ring into the spectrophotometrically detectable formazan by mitochondrial dehydrogenases.¹² Cells were seeded in 96-well plates at 8×10^3 cells/well to obtain optimal cell density throughout the experiment. After treatment of cells with test compounds for 24 h, the MTT solution (0.5%, 20 μ L) was added to each well. Following incubation at 37 °C for 3 h, the supernatant was removed and replaced with 100 μ L of DMSO to solubilize formazan crystals. The optical density of each sample in the well was then measured with a microplate spectrophotometer reader (Digital and Analog Systems, Rome, Italy) at $\lambda=550$ nm, and cell viability calculated as percentage respect to untreated controls. Each experiment in quadruplicate wells was repeated at least two times, and the mean \pm SD for each value was calculated. IC_{50} values have been calculated with GraphPad Prism 5 for Windows using a nonlinear fit transform sigmoidal dose-response (variable slope).

Western Blot Analysis

MCF-7 cells were harvested using cell lysis buffer; cell lysates were collected for Western blot analysis as previously described.¹³ The membranes were incubated with the primary antibody against σ_1 receptor, purchased from Thermo Fisher Scientific (Waltham, MA USA). The complex protein–primary antibody was detected using secondary horseradish peroxidase-conjugated anti-rabbit, and the chemiluminescence signal was captured using the Gel Logic 2200 Imaging System.

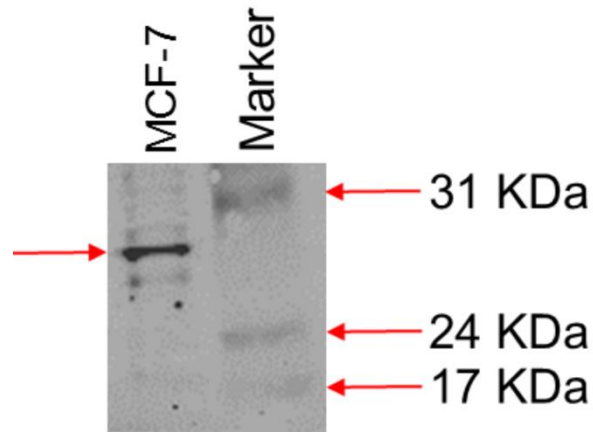


Figure S4: Representative immunoblotting image of σ_1 receptor detected in MCF-7 cells line by specific primary antibody (Thermo Fisher Scientific, PA5-30372).

NMR spectra

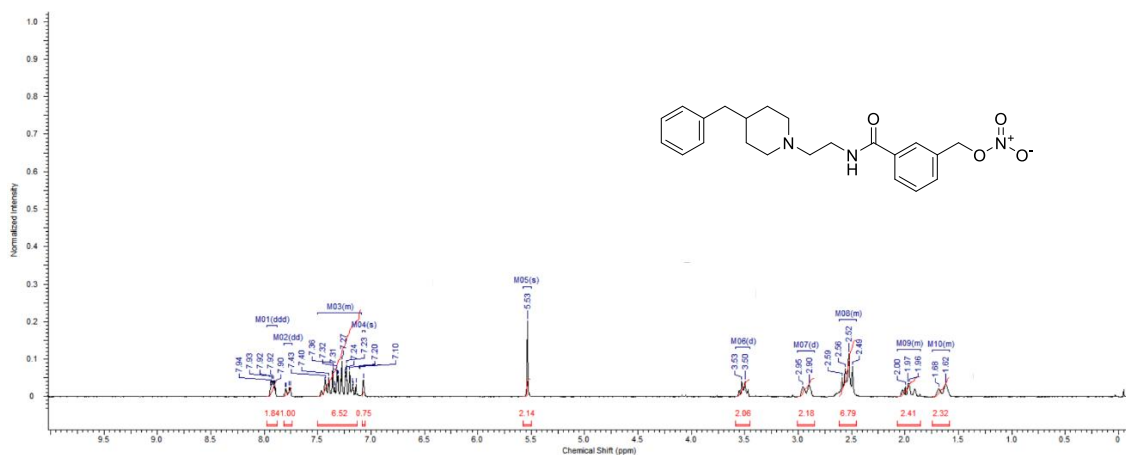


Figure S5 ^1H NMR-spectrum in CDCl_3 of 3-((2-(4-benzylpiperidin-1-yl)ethyl)carbamoyl)benzyl nitrate (9)

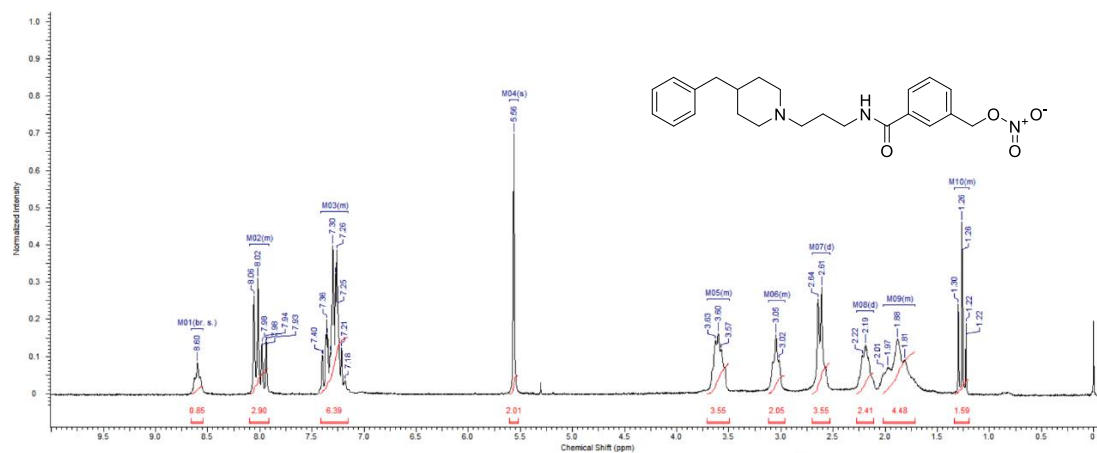


Figure S6 ^1H NMR-spectrum in CDCl_3 of 3-((3-(4-benzylpiperidin-1-yl)propyl)carbamoyl)benzyl nitrate (10)

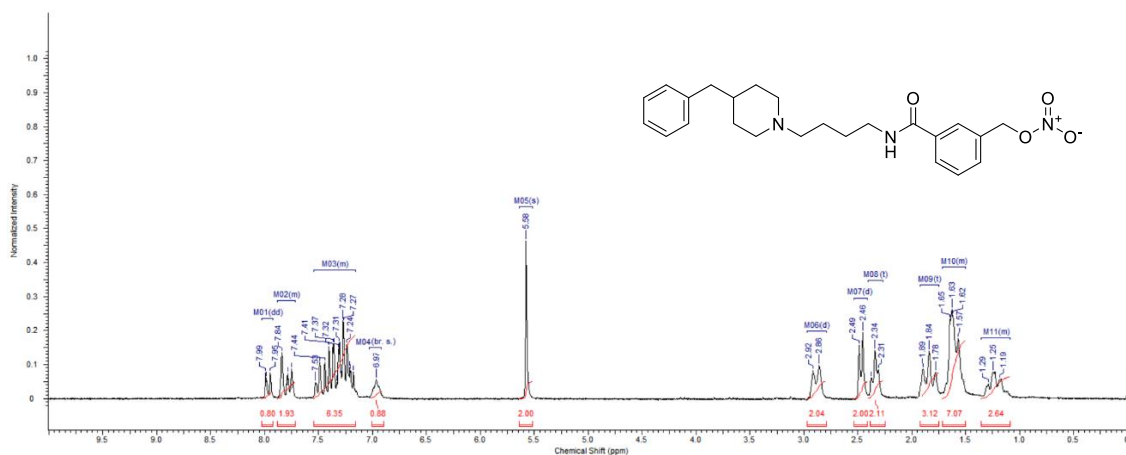


Figure S7 ^1H NMR-spectrum in CDCl_3 of 3-((4-(4-benzylpiperidin-1-yl)butyl)carbamoyl)benzyl nitrate (11)

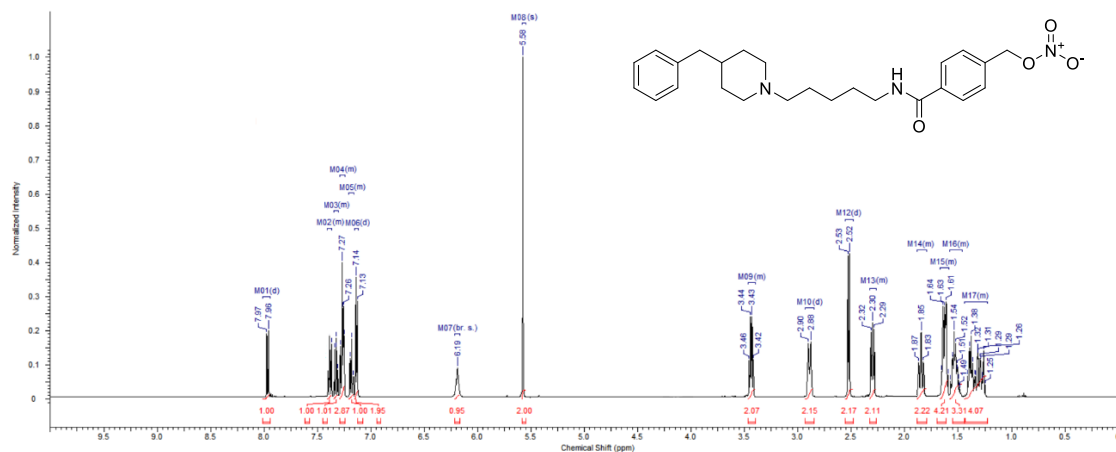


Figure S8 ^1H NMR-spectrum in CDCl_3 of 4-((5-(4-benzylpiperidin-1-yl)pentyl)carbamoyl)benzyl nitrate (**12**)

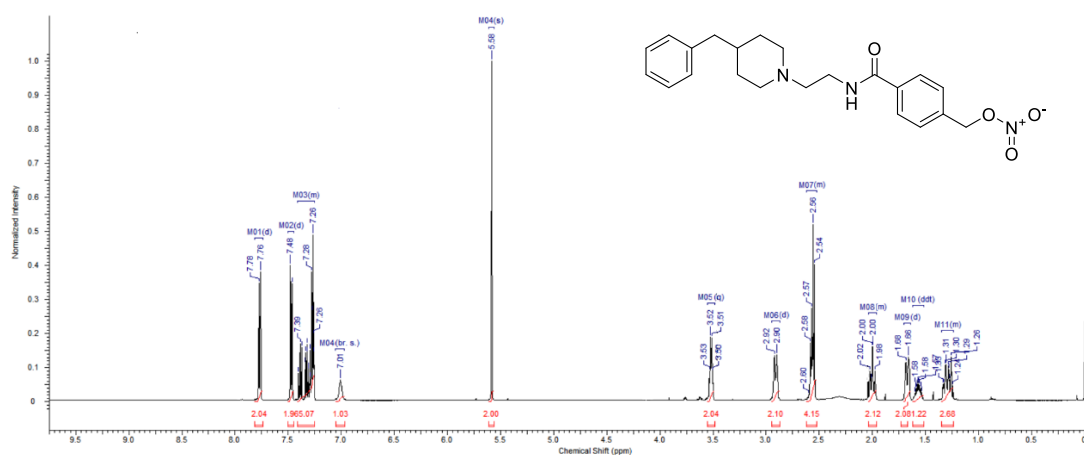


Figure S9 ^1H NMR-spectrum in CDCl_3 of 4-((2-(4-benzylpiperidin-1-yl)ethyl)carbamoyl)benzyl nitrate (**13**)

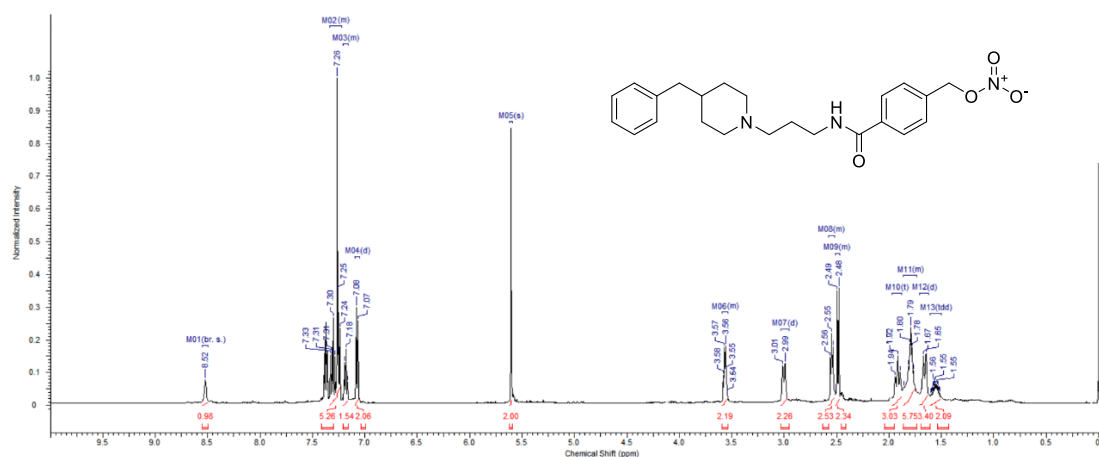


Figure S10 ^1H NMR-spectrum in CDCl_3 of 4-((3-(4-benzylpiperidin-1-yl)propyl)carbamoyl)benzyl nitrate (**14**)

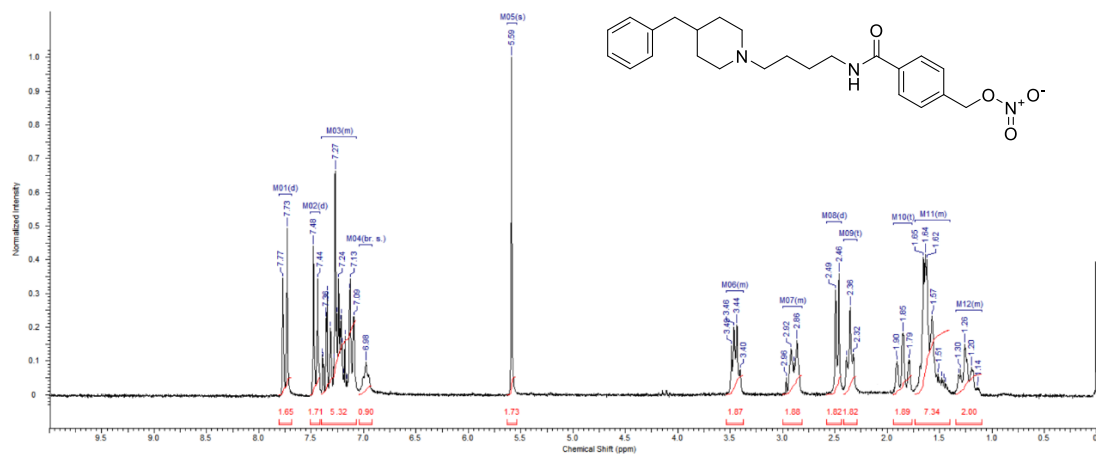


Figure S11 ¹H NMR-spectrum in CDCl₃ of 4-((4-(4-benzylpiperidin-1-yl)butyl)carbamoyl)benzyl nitrate (15)

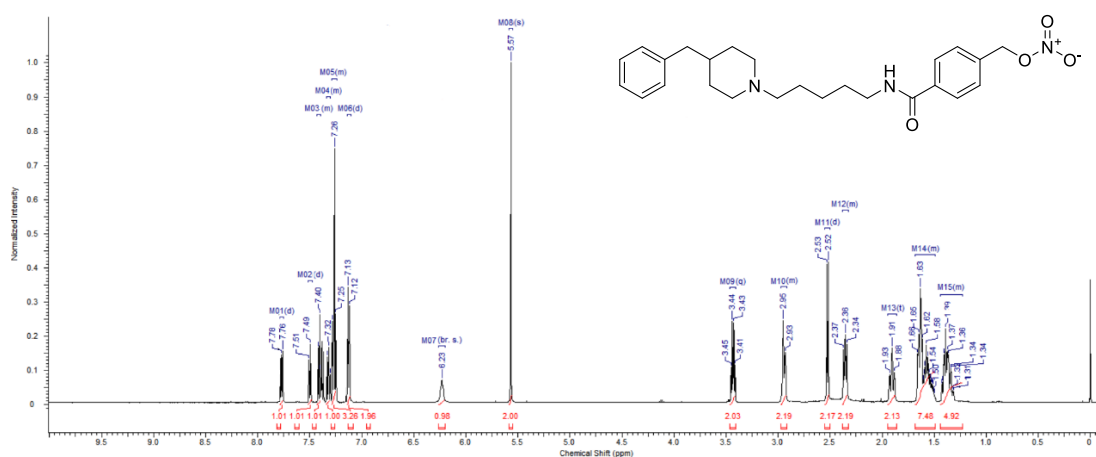


Figure S12 ¹H NMR-spectrum in CDCl₃ of 4-((5-(4-benzylpiperidin-1-yl)pentyl)carbamoyl)benzyl nitrate (16)

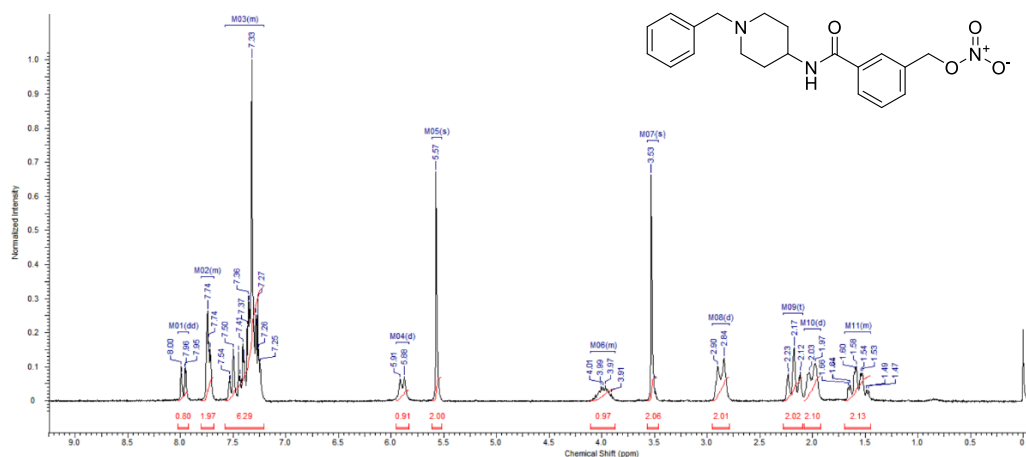


Figure S13 ¹H NMR-spectrum in CDCl₃ of 3-((1-benzylpiperidin-4-yl)carbamoyl)benzyl nitrate (17)

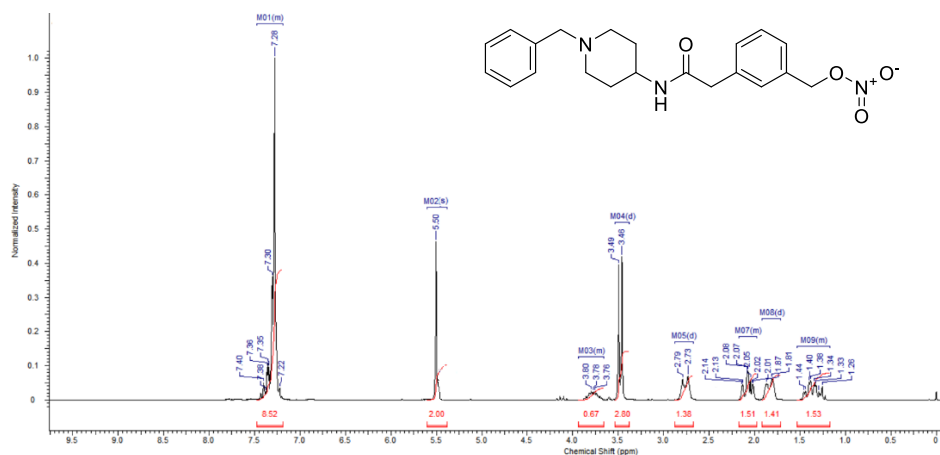


Figure S14 ¹H NMR-spectrum in CDCl₃ of 3-(2-((1-benzylpiperidin-4-yl)amino)-2-oxoethyl)benzyl nitrate (**18**)

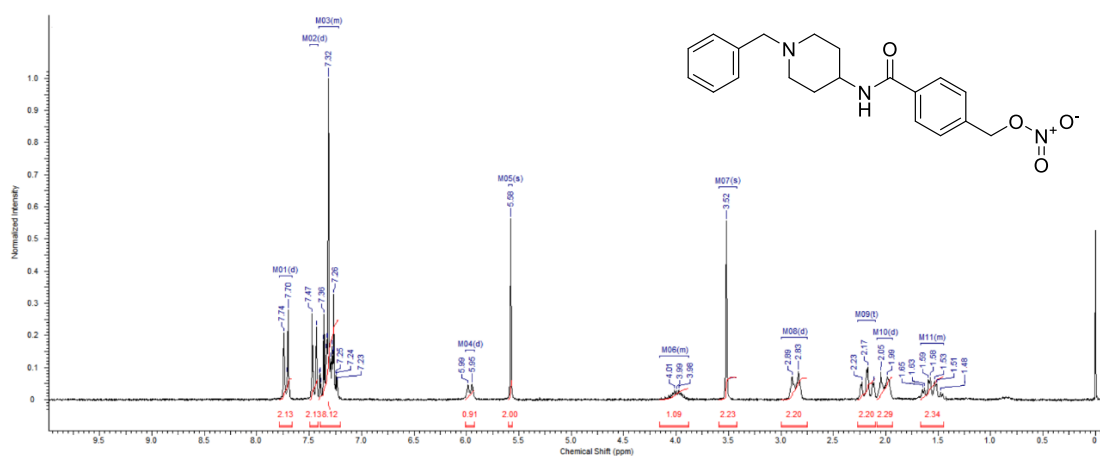


Figure S15 ¹H NMR-spectrum in CDCl₃ of 4-((1-benzylpiperidin-4-yl)carbamoyl)benzyl nitrate (**19**)

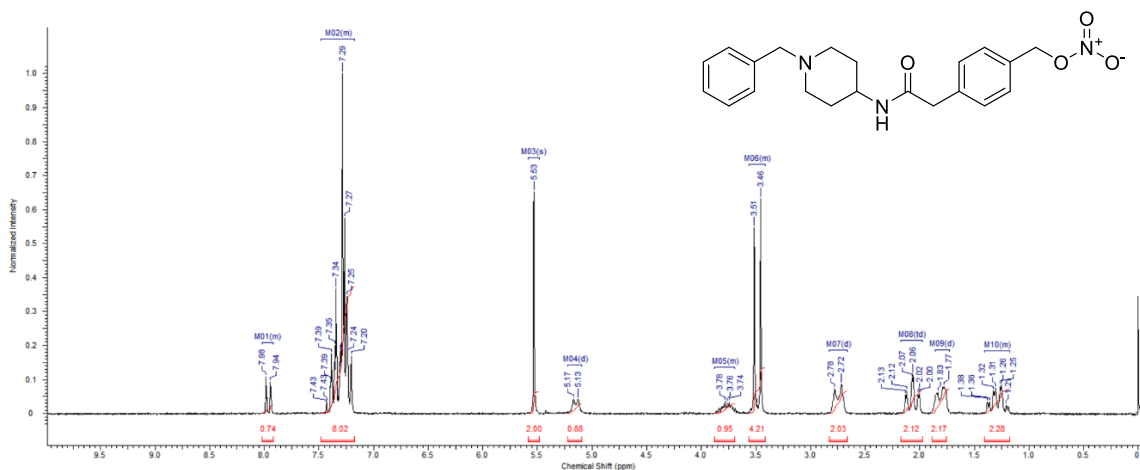


Figure S16 ¹H NMR-spectrum in CDCl₃ of 4-(2-((1-benzylpiperidin-4-yl)amino)-2-oxoethyl)benzyl nitrate (**20**)

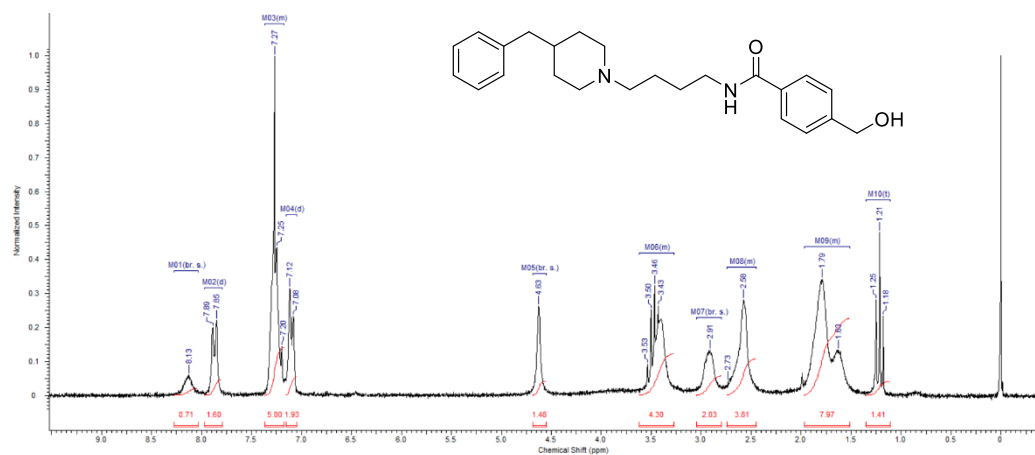


Figure S17 ^1H NMR-spectrum in CDCl_3 of *N*-(4-(4-benzylpiperidin-1-yl)butyl)-4-(hydroxymethyl)benzamide (**23a**)

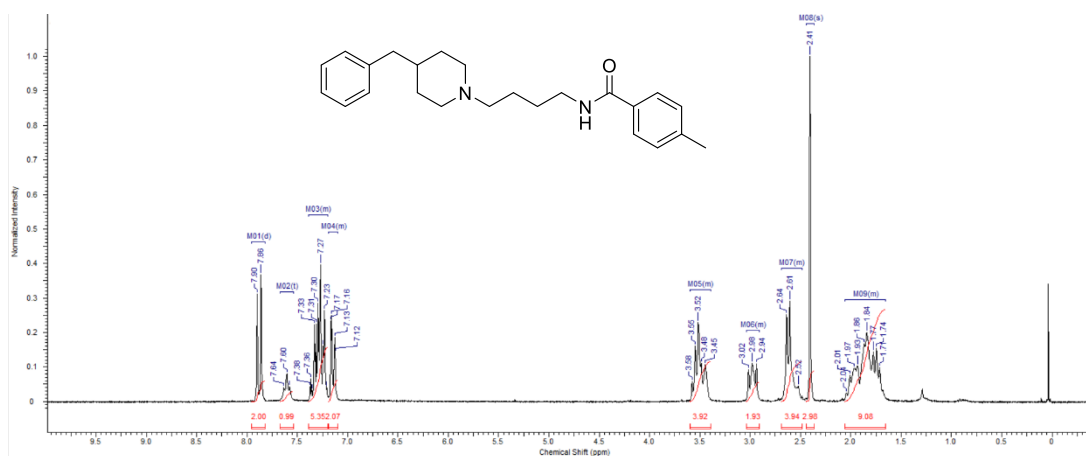


Figure S18 ^1H NMR-spectrum in CDCl_3 of *N*-(4-(4-benzylpiperidin-1-yl)butyl)-4-methylbenzamide (**23b**)

References

- (1) Krieger, E.; Koraimann, G.; Vriend, G., Increasing the precision of comparative models with YASARA NOVA--a self-parameterizing force field. *Proteins* **2002**, *47*, 393-402.
- (2) Krieger, E.; Vriend, G., YASARA View - molecular graphics for all devices - from smartphones to workstations. *Bioinformatics* **2014**, *30*, 2981-2982.
- (3) Floresta, G.; Amata, E.; Barbaraci, C.; Gentile, D.; Turnaturi, R.; Marrazzo, A.; Rescifina, A., A Structure- and Ligand-Based Virtual Screening of a Database of "Small" Marine Natural Products for the Identification of "Blue" Sigma-2 Receptor Ligands. *Mar. Drugs* **2018**, *16*.
- (4) Stewart, J. J., Optimization of parameters for semiempirical methods V: modification of NDDO approximations and application to 70 elements. *J. Mol. Model* **2007**, *13*, 1173-1213.
- (5) Stewart, J. J. P., MOPAC2016. **2017**.
- (6) Krieger, E.; Nielsen, J. E.; Spronk, C. A.; Vriend, G., Fast empirical pKa prediction by Ewald summation. *J. Mol. Graph. Model* **2006**, *25*, 481-486.
- (7) Krieger, E.; Dunbrack, R. L., Jr.; Hoofst, R. W.; Krieger, B., Assignment of protonation states in proteins and ligands: combining pKa prediction with hydrogen bonding network optimization. *Methods Mol. Biol.* **2012**, *819*, 405-421.
- (8) DeHaven-Hudkins, D. L.; Fleissner, L. C.; Ford-Rice, F. Y., Characterization of the binding of [³H](+)-pentazocine to sigma recognition sites in guinea pig brain. *Eur. J. Pharmacol.* **1992**, *227*, 371-378.
- (9) Mach, R. H.; Smith, C. R.; Childers, S. R., Ibogaine possesses a selective affinity for sigma 2 receptors. *Life Sci.* **1995**, *57*, P157-62.
- (10) Griess, P., Bemerkungen zu der abhandlung der H.H. Weselsky und Benedikt "Ueber einige azoverbindungen". *Ber. Dtsch. Chem. Ges.* **1879**, *12*.
- (11) Amata, E.; Dichiaro, M.; Arena, E.; Pittalà, V.; Pitarà, V.; Cardile, V.; Graziano, A. C. E.; Fraix, A.; A., M.; Sortino, S.; Prezzavento, O., Novel sigma receptors ligands-nitric oxide photodonor: molecular hybrids for double-targeted antiproliferative effect. *J. Med. Chem.* **2017**, *60*, 9531-9544.
- (12) Acquaviva, R.; Sorrenti, V.; Santangelo, R.; Cardile, V.; Tomasello, B.; Malfa, G.; Vanella, L.; Amodeo, A.; Genovese, C.; Mastrojeni, S.; Pugliese, M.; Ragusa, M.; Di Giacomo, C., Effects of an extract of *Celtis aetnensis* (Tornab.) Strobl twigs on human colon cancer cell cultures. *Oncol. Rep.* **2016**, *36*, 2298-2304.
- (13) Malfa, G. A.; Tomasello, B.; Acquaviva, R.; Genovese, C.; La Mantia, A.; Cammarata, F. P.; Ragusa, M.; Renis, M.; Di Giacomo, C., *Betula etnensis* Raf. (Betulaceae) Extract Induced HO-1 Expression and Ferroptosis Cell Death in Human Colon Cancer Cells. *Int. J. Mol. Sci.* **2019**, *20*, E2723.